Research Performance Progress Report

SUBMITTED TO

U. S. Department of Energy
National Energy Technology Laboratory

WORK PERFORMED UNDER AGREEMENT

DE-FE0013919

Project title: **Mechanisms for Methane Transport and Hydrate Accumulation in Coarse-Grained Reservoirs**

SUBMITTED BY
Prof. Hugh Daigle, PI
Phone: 512-471-3775
Fax: 512-471-9605
daigle@austin.utexas.edu

April 28, 2016

DUNS number: 1702302390000

RECIPIENT ORGANIZATION
University of Texas at Austin
200 E Dean Keeton St., Stop C0300
Austin, TX 78712-1585

PROJECT PERIOD: October 1, 2013 – September 30, 2017

REPORTING PERIOD END DATE: March 31, 2016

REPORT FREQUENCY: Quarterly

Signed:

Hugh Daigle

ACCOMPLISHMENTS

The project **goal** is to show, through numerical modeling, how the transport of methane, and the mechanism by which it is transported, control the development of persistent, massive hydrate accumulations in deep sediments below the seabed. The models will be based on recently collected data from Walker Ridge Block 313 (WR 313) in the northern Gulf of Mexico (Figure 1). To achieve the project goal, the project has been divided into three phases. Phase 1 of the project will focus on modifying an existing reservoir simulator (Sun and Mohanty, 2006) to include microbial methane production, salt mass balance and effects on methane stability, and sedimentation. Additional 1-D modeling will provide constraints on expected rates of methanogenesis. Phase 2 of the project will focus on simulations of dissolved methane migration mechanisms to determine if sufficient flux is available to develop the massive hydrate accumulations observed at WR 313. Phase 3 of the project will focus on simulations of free methane gas migration and recycling of methane in the gas phase as it is buried below the base of the methane hydrate stability zone.

The **objectives** of this project are to define:

1. The dissolved methane flux, organic matter abundance, and time required to develop the accumulations observed at WR 313 by short-distance migration of microbial methane into adjacent coarser-grained layers;
2. The dissolved methane flux and time required to develop the accumulations observed at WR 313 by long-distance, updip migration;
3. Whether there is enough methane in the dissolved phase in the fine-grained sediments to form the observed hydrate deposits or whether a gas phase is present, and if so what the conditions are for three-phase equilibrium;
4. The fate of hydrate that subsides beneath the base of the MHSZ and accumulates as gas, and overpressure generation associated with gas accumulation.

Tasks to be performed

PHASE 1 / BUDGET PERIOD 1

Task 1 - Project management and planning

The Recipient shall work together with the DOE project officer upon award to develop a project management plan (PMP). The PMP shall be submitted within 30 days of the award. The DOE Project Officer shall have 20 calendar days from receipt of the PMP to review and provide comments to the Recipient. Within 15 calendar days after receipt of the DOE's comments, the Recipient shall submit a final PMP to the DOE Project Officer for review and approval.

The Recipient shall review, update, and amend the PMP (as requested by the DOE Project Officer) at key points in the project, notably at each go/no-go decision point and upon schedule variances of more than 3 months and cost variances of more than 10%, which require amendments to the agreement and constitutes a re-base lining of the project.

The PMP shall define the approach to management of the project and include information relative to project risk, timelines, milestones, funding and cost plans, and decision-point success criteria. The Recipient shall execute the project in accordance with the approved PMP covering the entire project period. The Recipient shall manage and control project activities in accordance with their established processes and procedures to ensure subtasks and tasks are completed within schedule and budget constraints defined by the PMP. This includes tracking and reporting progress and project risks to DOE and other stakeholders.

Task 2 – Reservoir Model Development

The Recipient shall modify an existing general purpose reservoir simulator to include sedimentation, microbial methane production and effect of salt on hydrate equilibrium. The methane equilibrium calculation shall be modified to include changes in water activity due to dissolved salt following the method of Handa (1990). The mass conservation calculation shall be modified to include sedimentation, burial, and changes in porosity over time following the method of Bhatnagar et al. (2007). The initial conditions shall be modified to allow specification of heterogeneous properties (e.g., porosity) throughout the model domain. The boundary conditions shall be modified to allow specification of seafloor sedimentation rate and fluid flux. The Recipient shall verify code modifications with benchmark comparisons of performance with published simulation results (e.g., Bhatnagar et al., 2007).

Task 3 – 1-D Modeling of Microbial Methanogenesis

Concurrently with Task 2, the Recipient shall start with a 1-D reaction-transport model that will follow the burial by sedimentation of a sand layer surrounded by fine-grained sediments. The time-dependent modeling shall track the evolution of gas hydrate formation in the sand layer and shall provide more accurate estimates of the time scales and of the gas hydrate quantities associated with short migration. The methane hydrate stability conditions shall include the effect of pore size in the sand and fine-grained layers following the method of Malinverno (2010). The rate and spatial distribution of microbial methanogenesis shall be constrained by data from scientific ocean drilling expeditions (DSDP, ODP, IODP). The results of this task shall provide first-order constraints on rates of methanogenesis which shall be used as inputs to subsequent tasks (4.1, 4.3, 5.1, 5.2).

PHASE 2 / BUDGET PERIOD 2
Task 4.1 – Short Migration of Dissolved Methane

The Recipient shall investigate short migration of dissolved methane, in which methane generated in fine-grained sediments within the MHSZ is transported by diffusion into adjacent coarse-grained layers in which it forms concentrated hydrate deposits. The simulator developed in Task 2 shall be used for this task. The model domain shall consist of dipping sand layers surrounded by fine-grained sediments. This domain shall be designed to approximate the geometries observed at WR313 with sediment physical properties defined from logs or analog data. Rates of microbial methanogenesis and fluid flow shall be altered to determine the effect each has on the resulting hydrate distribution and time required for accumulation. The model results shall be used to determine the time scale of short migration at WR313, and the distribution of hydrate resulting from short migration.

Task 4.2 – Long Migration of Dissolved Methane

The Recipient shall investigate long migration of dissolved methane, in which dissolved methane is transported by advection from a distant source to the MHSZ. The investigation shall use the simulator developed in Task 2. The model domain shall consist of dipping sand layers surrounded by fine-grained sediments, and shall be designed to approximate the geometries observed at WR313. The model shall assume no local methane generation in the MHSZ and pore water entering the MHSZ with a methane concentration equal to the local solubility. Fluid flux shall be determined assuming that fluid flow is driven by overpressures to due high sedimentation rates (Gordon and Flemings, 1998). The Recipient shall explore the time scale associated with long migration by determining how long is required for fluid flow to form hydrate deposits comparable to those observed at WR313. The Recipient shall additionally simulate situations in which active fluid flow ceases after some time, and investigate how the hydrate that is formed evolves after cessation of fluid flow.

Task 4.3 – Assessment of Flux Associated with Dissolved Methane Migration

The Recipient shall use the model results from Tasks 4.1 and 4.2 to assess the methane flux associated with methane migration in the dissolved phase by either long or short migration. The different scenarios modeled in Tasks 4.1 and 4.2 shall be analyzed to determine methane flux from each migration mechanism, and the time scales and hydrate volumes produced by each. The analysis results shall be compared to the observed hydrate accumulations at WR313 and the age of the host sediments to determine whether migration of dissolved methane could have produced the observed hydrate accumulations.

PHASE 3 / BUDGET PERIOD 3

Task 5.1 – Assessment of Methane Budget Required for Presence of Gas Phase

The Recipient shall use the results of Tasks 4.1 and 4.2 to define methane availability from local, microbial sources as well as deeper sources (thermogenic or microbial). The phase equilibrium implemented in the 3-D model in Task 2 shall be used to determine local solubility within the model domain and determine the amount of methane that may be present as a gas phase. The results of this task will be used to place limits on gas availability in Tasks 5.2 and 5.3.

Task 5.2 – Free Gas Migration

The Recipient shall apply a previously established model of hydrate formation (multiphase-flow-controlled, nonequilibrium, neglecting transport of salinity and latent heat) to assess whether the gas phase accumulated beneath the MHSZ can contribute significantly to hydrate saturations within the MHSZ. The Recipient shall evaluate the conditions under which the accumulated gas phase drains into coarse-grained sediment. Having identified those conditions, the Recipient shall evaluate the geologic setting (dip angle, petrophysical properties and multiphase flow properties of the sediment) for which significant updip migration of the gas phase can be expected. The Recipient shall apply the hydrate formation model to geologic settings with significant expected migration to determine the hydrate saturation distribution in the updip direction. The model shall be tested for ranges of the two competing rates (namely, rate of gas accumulation at base of MHSZ and rate of hydrate formation from gas phase and water phase in the MHSZ). The Recipient shall additionally determine the pressure, temperature, and salinity conditions that will permit short migration of a gas phase within the MHSZ. The predicted saturation distributions shall be compared to observations (magnitude of hydrate saturation and its lateral extent) within coarse-grained layers at WR313. If hydrate is predicted to form in the same location and same volume as the accumulations observed at WR313, the Recipient shall determine whether the conditions that give agreement are geologically plausible, and the Recipient shall compare the flux of methane in the gas phase to the fluxes of methane by other mechanisms to be determined in Tasks 4.1 and 4.2. If the rates of methane delivery and time scale of hydrate accumulation are consistent with the accumulations observed at WR313, the Recipient shall use the results to guide the inclusion of free-gas migration phenomena into the full-physics 3D simulations of Task 5.3.

Task 5.3 – Methane Recycling at the Base of the MHSZ

The Recipient shall use the reservoir model developed in Task 2 to evaluate the fate of hydrate that moves below the base of the MHSZ as a result of sedimentation. In particular, the Recipient shall examine subsidence of dipping, hydrate-bearing sands of the type encountered at WR313. The Recipient shall model burial of a dipping sand layer through the base of the MHSZ in 3 dimensions. The Recipient shall test different scenarios of sedimentation rate, hydrate saturation in sand layers, and deep methane flux to evaluate gas accumulation below the MHSZ, supply of methane to the base of the MHSZ, and overpressure generated by the accumulation of a connected gas column. The gas column will be considered connected when it overcomes a percolation threshold of roughly 10% of the pore volume (England et al., 1987). Gas phase pressure shall be computed from gas column height and estimates of capillary pressure from analog sediments (e.g., Blake Ridge; Clennell et al., 1999). The potential to fracture overlying sediments shall be investigated by comparing the resulting pore pressure to the total vertical stress and the minimum horizontal stress.

Milestone Status Report

1.A Title: PMP submission
Planned Date: 4 December 2013
Completed Date: 22 November 2013
Verification Method: Submission of final Project Management Plan to DOE within 65 days of start of project.

1.B Title: Project kick-off meeting
Planned Date: 29 December 2013
Completed Date: 7 November 2013
Verification Method: Meeting held within 90 days of start of project.

1.C Title: Sedimentation, microbial methane production, salinity effect implementation
Planned Date: 30 June 2014
Completed Date: 30 June 2014
Verification Method: Implementation of sedimentation, microbial methane production, salinity effect on hydrate stability in 3-D model.

1.D Title: Benchmarking of numerical model against published results
Planned Date: 31 March 2015
Completed Date: 31 March 2015
Verification Method: Simulation results match those obtained from other simulators in 1-D and 2-D (e.g., Bhatnagar et al., 2007; Chatterjee et al., 2011) within 1% in time and hydrate saturation using the same input parameters.

1.E Title: Development of time and methanogenesis constraints for future modeling
Planned Date: 31 March 2015
Completed Date: 31 March 2015
Verification Method: Development of a model that includes time-dependent changes in methane stability in a dipping, subsiding sand layer but matches the results of Cook and Malinverno (2013) for steady-state conditions.

2.A Title: Completion of short migration modeling
Planned Date: 30 September 2016
Verification Method: Completion of simulations to evaluate conditions necessary for development of massive hydrate deposits by short migration.

2.B Title: Completion of long migration modeling
Planned Date: 30 September 2016
Verification Method: Completion of simulations to evaluate conditions necessary for development of massive hydrate accumulations by long migration.

2.C Title: Quantification of methane flux in the dissolved phase
Planned Date: 30 September 2016
Verification Method: Quantification of methane flux associated with methane migration in the dissolved phase by either long or short migration and comparison with existing estimates of methane flux in the northern Gulf of Mexico such as those presented in Frye (2008).

3.A Title: Quantification of methane availability and expected quantities of gas
Planned Date: 30 September 2017
Verification Method: Quantification of amount of methane required to form a free gas phase and comparison with existing estimates of methane flux in the northern Gulf of Mexico such as those presented in Frye (2008).

3.B Title: Completion of free gas migration models
Planned Date: 30 September 2017
Verification Method: Determinations of methane flux and time necessary to reproduce observed hydrate accumulations at WR313 by migration of free gas.

3.C Title: Completion of modeling efforts to assess methane recycling
Planned Date: 30 September 2017
Verification Method: Completion of simulations to assess rates of gas accumulation beneath MSHZ and effect on gas migration and overpressure generation.

What was accomplished under these goals?

Major activities

<u>Task 4.1.</u>

Li Wei started as a PhD student on the project working on 1D numerical modeling in January 2016. Li has already achieved basic model construction and we are currently able to observe the differences in methane concentration and hydrate distribution between homogenous sedimentary environments and environments with single or multiple sand layers.

Malinverno implemented a time-dependent reaction-transport model to calculate gas hydrate content. This model allows for exploring how temporal variations in the deposition of organic carbon at the seafloor can impact gas hydrate formation in the sediment column. These variations in organic carbon content may explain the occurrence of discrete fine-grained sediment intervals with hydrate in veins and fractures. These fractured intervals are not connected to potential methane sources below the hydrate stability zone and therefore are likely sourced from microbial methane. The results will provide boundary conditions to test whether diffusion of microbial methane can generate significant hydrate accumulation in coarse-grained layers.

Daigle and Nole have been working on 3-D basin modeling of hydrate accumulation in sand layers like those encountered at Walker Ridge Block 313. A significant challenge to accurate basin-scale modeling of reactive transport in porous media is the inability to sufficiently resolve important heterogeneities in a simulation domain that spans multiple kilometers in all directions. In shallow hydrate-bearing sands typical of those encountered in the Terrebonne Basin in the Gulf of Mexico, sand layers are commonly only about 3 to 5 meters thick. In a simulation environment that involves time-dependent grid properties, grid blocks whose vertical discretization is on the order of 3m typically result in inefficient simulation runtime. The simulations performed in this study do not incorporate impacts of hydrate saturation on methane diffusivity. Therefore, because methane transport occurs primarily due to diffusion, hydrate accumulations in sandy layers only track diffusive mass transport, which should remain constant regardless of grid discretization if the discretization itself does not cause competition between sand layers for methane diffusion from clays.

To validate this idea, simulations are performed at two different sand layer discretizations on synthetic planar sands. Grid block thickness in both simulations is 18.31m in the vertical direction; in the first simulation, sands are one grid block thick, and in the second simulation sands are three grid blocks thick (54.93m thick). Depicted in Figure 1, the sum of the hydrate saturations within the sands between both simulations is approximately equal across both sand discretizations.

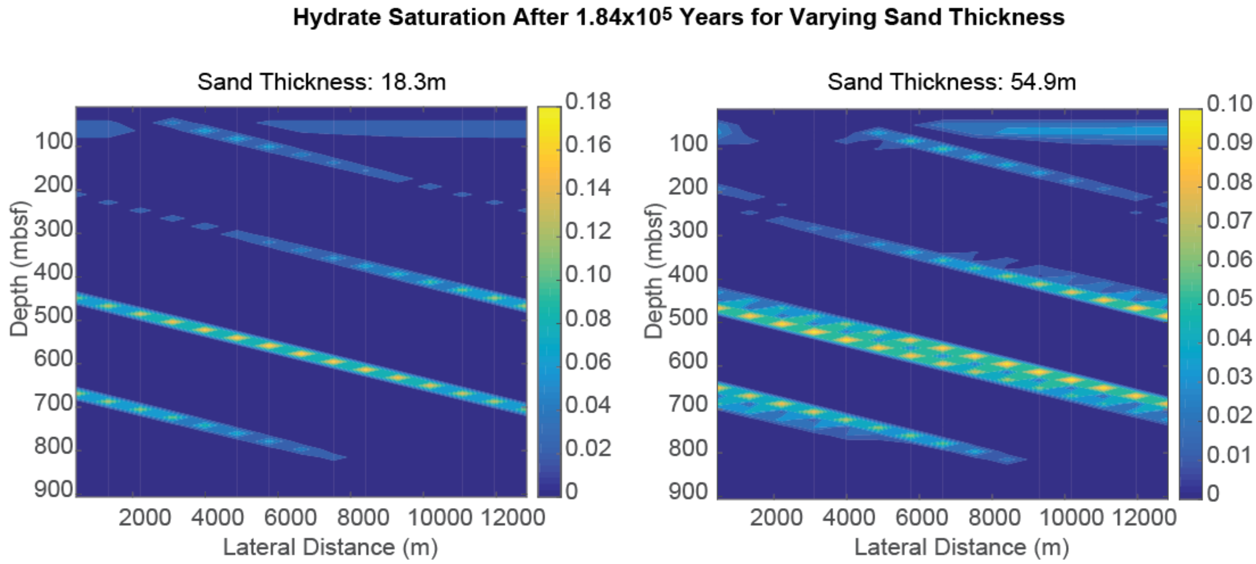

Figure 1. Variation in hydrate saturation within sand layers for different grid discretizations in a diffusive system.

On average over the entire 3D basin (118.74 km^3), the difference in total mass transport to all sand layers between both simulations is only 8.30%. Minor differences in total mass transport are due to the facts that a) solubility of methane changes more with depth across a thicker sand than a thinner sand, b) the methanogenesis source in the clay layers is stronger above and weaker below a thick sand simulation as compared to a thin sand simulation, c) there is a greater surface area in 3D upon which diffusion can act in the thicker sand than the thinner sand simply due to the fact that this simulator uses rectangular grid blocks, and d) simulation end times are slightly different due to time step varying based on convergence criteria. This result indicates that hydrate saturation distributions in coarse simulated sands can be scaled to approximate saturations that could be expected in thinner sands in nature.

Constraining Model Parameters with Core Samples and Log Data

While many significant input parameters to methane hydrate reservoir simulations can be estimated with a high degree of accuracy (such as geothermal gradient, sediment density, water depth, etc.), some physical parameters still remain highly uncertain. In particular, both the clay-sand pore size contrast and the reaction rate of methanogenesis remain challenging to constrain. The clay-sand pore size contrast is important because it dictates the strength of the diffusive gradient along which methane sourced in clayey intervals is transported toward sandy layers. The reaction rate of methanogenesis dictates the both the magnitude of methane sourcing in the sediment column at any particular time as well as how the methane source diminishes with depth.

To constrain the clay-sand pore size contrast throughout the depth of a basin, pore size distributions obtained experimentally from core samples can be tied to nuclear magnetic resonance (NMR) log data. Sand pores are typically large enough to not have a significant impact on methane solubility in comparison to bulk water methane solubility, so a constant value of 10 microns is assumed to represent sandy strata in simulations. In this study, NMR log data is mapped to clay pore size distributions by first performing mercury injection capillary pressure (MICP) measurements on core samples taken from Keathley Canyon Block 151. Mercury injection data for each core sample yields a pore throat size distribution, which is then compared to the NMR log signature at the well depth from which each sample was taken. The T_2 distribution from NMR data samples the surface area to volume ratio of sediment pore bodies as follows:

$$\frac{1}{T_2} \approx \rho \frac{S}{V}, \qquad \text{(Eq. 1)}$$

where T_2 is the surface relaxation time in milliseconds, ρ is the surface relaxivity of the porous rock [length/millisecond], S is the surface area of the pore space [length^2], and V is the volume of the pore space [length^3]. In the clayey samples, surface relaxivity is approximately 1.023 nm/millisecond.

In typical petrophysical applications, the pore bodies of sediments are assumed to be spherical when correlating T_2 distributions to pore sizes. The surface area to volume ratio can then be expressed simply in terms of one parameter, the pore radius. In clayey sediments, however, pore bodies are typically on the order of tens of nanometers and are highly elongated. To adequately model Gibbs-Thomson phase equilibrium phenomena, it is very important to try and respect pore geometry when characterizing pore size distributions of small pores. Therefore, this study employs a two-parameter pore size estimator, whereby pores are assumed to take the shape of oblate ellipsoids. Scanning electron microscope image analysis in 2D on clayey sediment samples yields clay pore circularities of approximately 0.2, on average (see Nole et al., 2016); assuming pores are ellipses in 2D and rotating about the major axis into 3D, the resulting ellipsoids can be characterized as having an aspect ratio between major (r_{max}) and minor (r_{min}) axes of 12:1. The surface area to volume ratio of the pore space can then be expressed as a function of r_{min} in nm as follows:

$$\frac{S}{V} \approx \frac{1.545}{r_{\min}}. \qquad \text{(Eq. 2)}$$

Mercury injection data can be used to tie physical pore sizes to an NMR distribution by assuming that the largest pore throat sampled by MICP experiments corresponds to the minor axis of a pore in an NMR distribution at two standard deviations above the mean pore size (Bihani et al., 2015). Using NMR log data at Walker Ridge, the mean and standard deviation of T_2 can be used to generate a lognormal distribution of T_2 values at every sampling depth within the log (approximately 0.15 m apart). This distribution is then mapped to an r_{min} pore size distribution via MICP data, and the r_{min} distribution can be converted to r_{max} via the aspect ratio. An example NMR pore size distribution calculated for Walker Ridge is depicted in Figure 2.

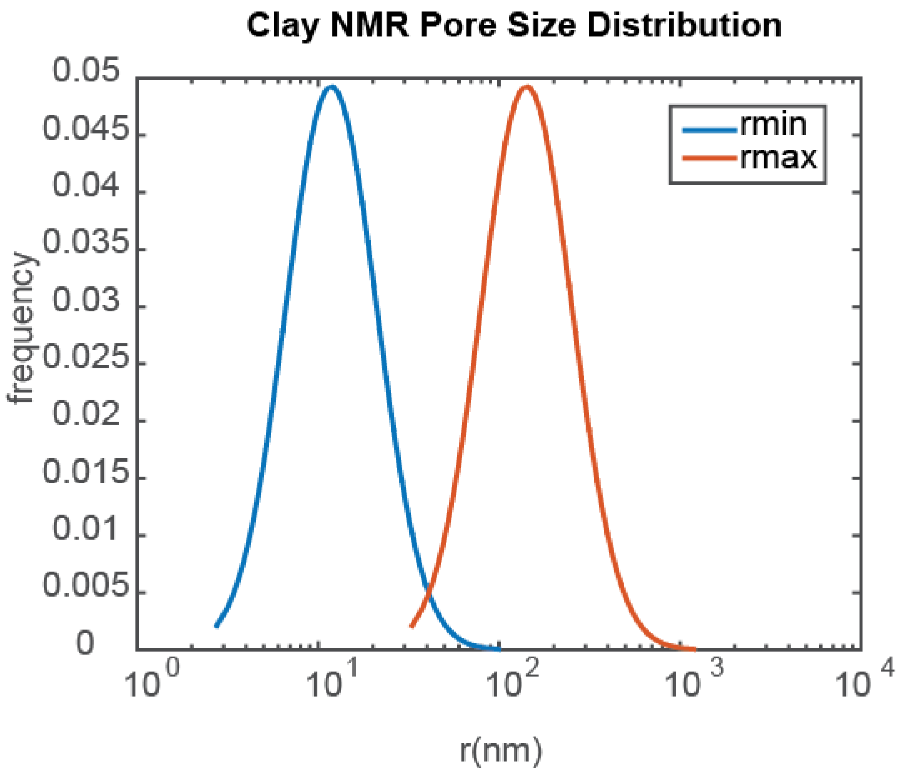

Figure 2. Example synthetic two-parameter NMR pore size distribution for a clayey interval.

The clay pore size distributions obtained from this analysis can be used to constrain the clay pore radius implemented in the simulator, which governs methane solubility, the strength of the diffusive gradient from clays to sands, and the nature of hydrate growth as either pore-filling or fracture-forming. The simulations performed in this study only consider pore-filling hydrate growth, but hydrofracturing due to hydrate growth is an area of future development. Hydrate tends to nucleate within pores as a spherical mass; therefore in oblate ellipsoidal pores, interstitial hydrate growth should be limited by the minor axis of the pore, r_{min}. Analysis of NMR log data at Walker Ridge suggests median clay minor axis radii of about 10 nm, which is employed as the clay pore radius governing methane solubility in these simulations.

This study constrains the rate of methanogenesis by comparing observations of hydrate accumulations throughout the Terrebonne Basin to the potential hydrate growth mode in the clays within the basin, which is dictated by the stress state of the system and the clay pore sizes.

Adapting the method of Henry et al. (1999) to the oblate ellipsoid model, the capillary pressure associated with the curvature of a precipitating hydrate phase determines whether hydrate growth will produce fractures or occur interstitially. A critical radius r_c can be defined as the pore radius below which hydrate growth will produce fractures (the pressure of the nonwetting phase due to capillarity exceeds the minimum principal effective stress) and above which hydrate will grow within the pore space, as follows:

$$r_c = \left(1 + \frac{r_{\min}}{r_{\max}}\right) \frac{\sigma_{sl}}{K\left(P_{lith} - P_{hyd}\right)}, \quad \text{(Eq. 3)}$$

where K is the ratio of minimum to maximum principal effective stress, σ_{sl} is the water-hydrate interfacial tension, P_{lith} is the lithostatic stress, and P_{hyd} is the hydrostatic pressure. Figure 3 depicts a depth-wise trend of the approximate pore radius at which hydrate growth changes from interstitial to fracture-filling, adjusting the lithostatic stress for porosity changes captured by log data. The Terrebonne Basin resides in an extensional tectonic setting, so K of 0.3 was selected to reflect slight unloading in the horizontal direction. Lithostatic and hydrostatic pressures were calculated using Walker Ridge parameters listed in Table 1. This is a first order approximation, as seafloor depth varies across the extent of the basin and sediment density varies with depth.

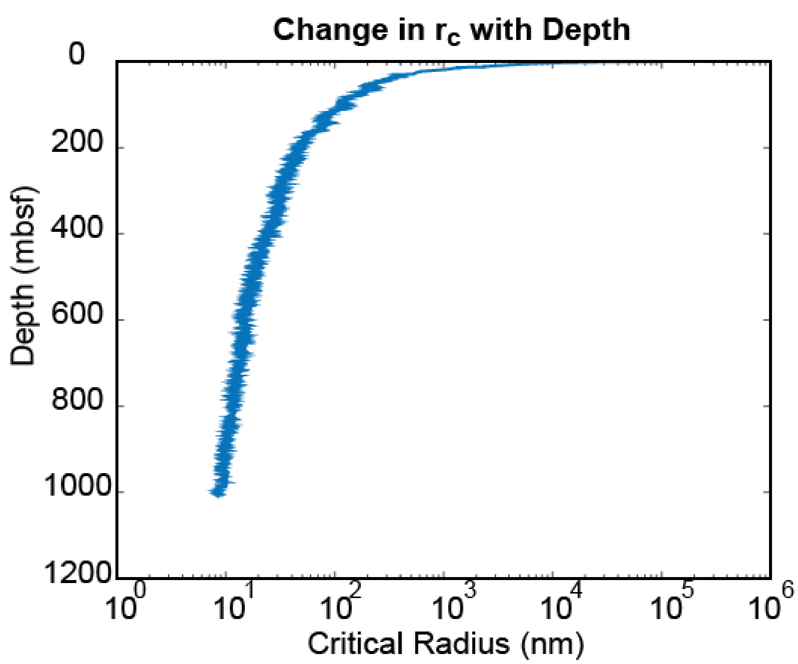

Figure 3. Change in critical pore radius with depth

Water depth	1917 m
Base of gas hydrate stability (BGHS)	841 mbsf
Geothermal gradient	19 ^{o}C/km
k_{α}	4482 kg/m^3
λ	10^{-12} s^{-1}
α_{BSRZ}	0.5%
ω	1 mm/yr
z_{BSRZ}	4.5 mbsf
r_{sand}	10 microns
r_{clay}	10 nm

Table 1. Walker Ridge Site 313 in-situ characteristics. Water depth, BGHS, and geothermal gradient from Hutchinson et al. (2008), and steady-state methanogenesis parameters from Malinverno (2010).

Integrating this analysis with clay pore size distributions constrained from NMR data, this study estimates the volume fraction of pore space that would fill with hydrate interstitially and the volume fraction of pore space that would fill as fractures, were methane to exceed solubility in all the pore space. It is important to note that in a situation where methane concentration increases from below the solubility of the largest pores, the largest pores would fill with hydrate first, followed by the smaller pores. Therefore, if any pore space were accessible to interstitially filling hydrate, hydrate would first precipitate within the larger pore space before generating fractures in the smaller pores.

Figure 4 compares pore size distributions from NMR data to the critical fracture radius, r_c. At shallow depths up to about 180 mbsf, hydrate growing in clays can only form fractures due to the stress state and pore sizes in the sediments. Beneath 180 mbsf, the fraction of pore space in which hydrate can form interstitially begins to increase until about 500 mbsf, beneath which point methane in excess of solubility cannot form fractures in any fraction of the pore space.

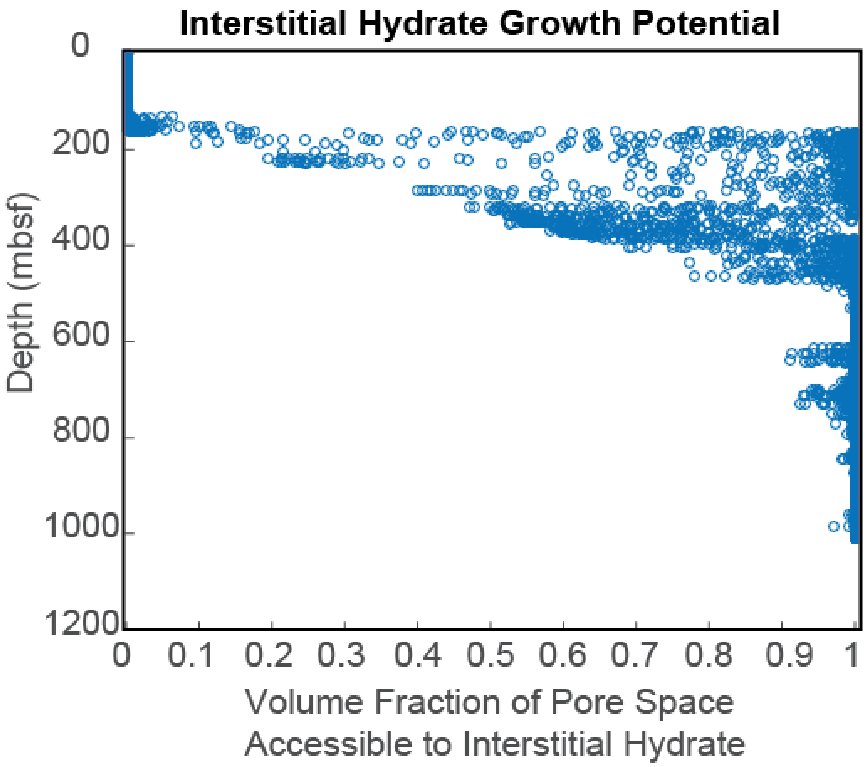

Figure 4. Interstitial hydrate growth potential in clayey intervals using NMR log-interpreted pore size distributions

This illustration is instructive when considering observations of methane hydrate accumulations in clays throughout this region. Methane hydrate is observed to exist only in fractures throughout the methane hydrate stability zone in the Terrebonne Basin, and it is largely absent as pore-filling hydrate in clays. In the region beneath 500 mbsf, it is impossible for hydrate to form fractures when methane concentration exceeds solubility; therefore, hydrate fractures beneath 500 mbsf must have been formed shallower before being buried. Additionally, because hydrate will fill pores interstitially before forming fractures, if methane concentrations exceed solubility in the clays between 180 mbsf and 500 mbsf, hydrate in fractures should coexist with hydrate filling pores. This coexistence is not observed in seismic or well log data, so it is likely that all fractured intervals beneath 180 mbsf had first formed above 180 mbsf and were subsequently buried.

Knowing the maximum depth at which methane concentration exceeds solubility in clays helps to constrain the rate at which methane can be supplied to the system via methanogenesis. Illustrated in Figure 5, methanogenesis sourcing to the simulations run in this study is expressed as a steady state, exponentially decaying function of depth. A higher methanogenesis reaction rate leads to a methanogenesis source that supplies more methane shallower in the column and decays faster with depth than a slower rate. Implementing a methanogenesis rate, λ, of 1×10^{-12} s^{-1} (about an order of magnitude greater than that estimated in Malinverno, 2010), organic methane flux decays by more than 95% by 200 mbsf, the point at which methane input should no longer be large enough to exceed solubility in clays. This methanogenesis rate is therefore implemented in simulations involving the Terrebonne Basin sand strata in order to provide more easily interpretable results of hydrate accumulations.

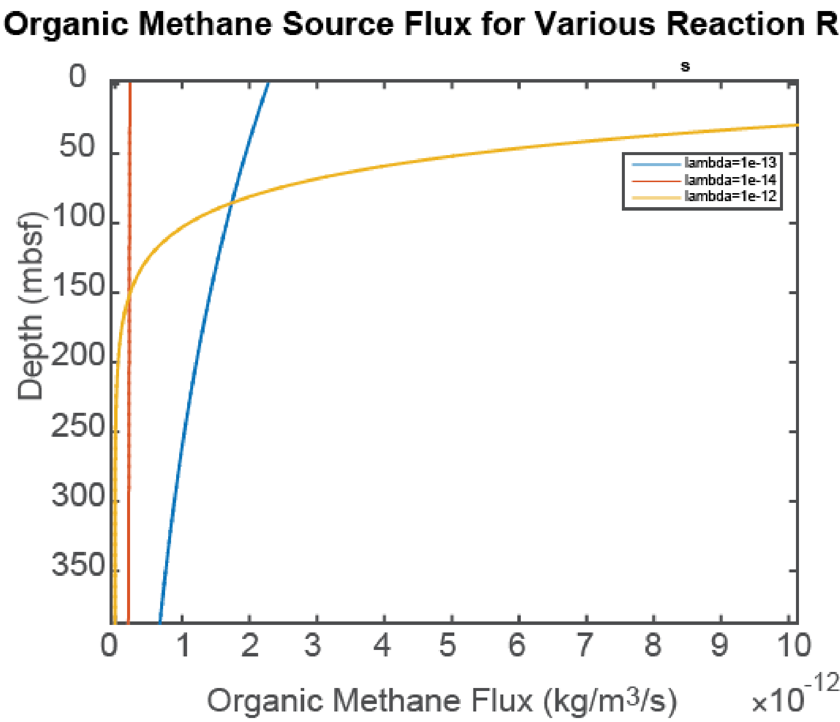

Figure 5. Methanogenesis source flux for various rates of microbial activity

<u>Task 4.2.</u> Nole is currently working on modeling advective cases. In particular, he is investigating the effect of overpressure on driving fluid flow back up through sands and either redistributing biogenic methane or delivering methane from a deeper source to the MHSZ.

<u>Task 4.3.</u> Results of this task are pending the outcome of the results of Task 4.2.

Specific objectives

None for this quarter.

Significant results and key outcomes

We have refined our petrophysical understanding of the physical properties of sediments at Walker Ridge. This has allowed us to better constrain the depths at which hydrate may form in the pore space of sediments or in fractures.

What opportunities for training and professional development has the project provided?

PI Daigle and co-PI Mohanty have been working with PhD student Michael Nole and MS students Ryan Andris, Abhishek Bihani, and Arash Shushtarian on various aspects of pore-scale modeling of methane hydrate systems. This work has involved weekly meetings and independent work.

Co-PIs Cook and Malinverno have been working with PhD student Li Wei on modeling microbial methanogenesis. This work has involved weekly meetings and independent work.

How have the results been disseminated to communities of interest?

Five abstracts were presentated at the American Geophysical Union Fall Meeting in December.

Plans during next reporting period to accomplish goals

Work will continue on Tasks 4.1, 4.2, and 4.3. In particular, we will focus on parameter space testing for diffusive and advective methane supply.

<u>PRODUCTS</u>

Andris, R., 2016. The effect of restrictive diffusion on hydrate growth. Gordon Research Conference on Natural Gas Hydrate Systems, Galveston, TX, 28 February – 4 March 2016. Published. Federal support acknowledged.

Hillman, J., 2016. Mapping and characterising bottom-simulating reflectors in 2D and 3D seismic data to investigate connections to lithology and frequency dependence. Gordon Research Conference on Natural Gas Hydrate Systems, Galveston, TX, 28 February – 4 March 2016. Published. Federal support acknowledged.

Malinverno, A., 2016. Modeling gas hydrate formation from microbial methane in the Terrebonne basin, Walker Ridge, Gulf of Mexico. Gordon Research Conference on Natural Gas Hydrate Systems, Galveston, TX, 28 February – 4 March 2016. Published. Federal support acknowledged.

Nole, M., 2016. Implications of pore-scale heterogeneities on biogenic methane hydrate distributions in marine sediments. Gordon Research Conference on Natural Gas Hydrate Systems, Galveston, TX, 28 February – 4 March 2016. Published. Federal support acknowledged.

Wei, L., 2016. A 1D mass balance model for the formation of gas hydrate in marine sequences. Gordon Research Conference on Natural Gas Hydrate Systems, Galveston, TX, 28 February – 4 March 2016. Published. Federal support acknowledged.

PARTICIPANTS AND OTHER COLLABORATING ORGANIZATIONS

Name: Hugh Daigle
Project role: PI
Nearest person month worked: 1
Contribution to project: Project management; assisted with code development
Collaborated with individual in foreign country: No

Name: Kishore Mohanty
Project role: Co-PI
Nearest person month worked: 1
Contribution to project: Assisted with code development
Collaborated with individual in foreign country: No

Name: Steven Bryant
Project role: Co-PI
Nearest person month worked: 1
Contribution to project: Assisted with code development
Collaborated with individual in foreign country: No

Name: Michael Nole
Project role: Graduate Student
Nearest person month worked: 3
Contribution to project: Primary worker on developing computer code
Collaborated with individual in foreign country: No

Name: Abhishek Bihani
Project role: Graduate Student
Nearest person month worked: 1
Contribution to project: Capillarity and phase equilibrium modeling
Collaborated with individual in foreign country: No

Name: Ryan Andris
Project role: Graduate Student
Nearest person month worked: 1
Contribution to project: Pore-scale diffusion modeling

Collaborated with individual in foreign country: No

Name: Ann Cook
Project role: Co-PI
Nearest person month worked: 1
Contribution to project: Worked on gathering specific data for modeling of microbial methanogenesis, developing methanogenesis code
Collaborated with individual in foreign country: No

Name: Li Wei
Project role: Graduate Student
Nearest person month worked: 3
Contribution to project: Worked on developing methanogenesis code
Collaborated with individual in foreign country: No

Name: Alberto Malinverno
Project role: Co-PI
Nearest person month worked: 1
Contribution to project: Provided data for microbial methanogenesis modeling
Collaborated with individual in foreign country: No

IMPACT

What is the impact on the development of the principal discipline of the project?

The central focus of this project is refining our understanding of the methane migration pathways that feed methane hydrate deposits in marine sediments. Understanding migration pathways is an important component of understanding methane hydrates as a petroleum system, a necessary step towards prospecting for economically recoverable hydrate deposits. Additionally, our results will help refine our understanding of the carbon cycle in marine sediments, and specifically how methane is transported and sequestered.

What is the impact on other disciplines?

The results of this project will be important for other engineering disciplines in which researchers are developing methods for extracting methane from the subsurface since it will provide information on how methane is distributed in sediments at different scales. In addition, the results will be of interest to the economics and risk assessment fields since we will develop methods to determine more precisely how much hydrate may be present in subsurface reservoirs.

What is the impact on the development of human resources?

This project will provide funding for three graduate students to conduct collaborative research on methane hydrates and give them an opportunity to participate in important hands-on learning experiences outside the classroom.

What is the impact on physical, institutional, and information resources that form infrastructure?

Our results may be used for better design of subsea oil and gas infrastructure since more precise assessment of hydrate resources will allow better assessment of hydrates as a hazard. In addition, production infrastructure specifically for hydrate reservoirs may be improved by our results since we will allow more accurate determination of the volumes of methane expected to exist in the subsurface.

What is the impact on technology transfer?

Our results will be disseminated at conferences and in peer-reviewed publications.

What is the impact on society beyond science and technology?

The impact of this work on society will be twofold. First, the better understanding of hydrates in a petroleum systems framework will allow for more efficient production of natural gas from these deposits, which will provide an additional energy resource. Second, the better understanding of methane cycling and distribution in the subsurface will influence regulatory decisions involving hydrates as geohazards or climate change agents.

What dollar amount of the award's budget is being spent in foreign country(ies)?
None

CHANGES/PROBLEMS
None

SPECIAL REPORTING REQUIREMENTS
None

BUDGETARY INFORMATION
See attached spreadsheet.

Variances: Still awaiting updated cost sharing information from subcontractors.

References

Bhatnagar, G., Chapman, W.G., Dickens, G.R., Dugan, B., Hirasaki, G.J., 2007. Generalization of gas hydrate distribution and saturation in marine sediments by scaling of thermodynamic and transport processes. Am. J. Sci., 307, 861-900.

Bihani, A., Daigle, H., Cook, A., Glosser, D., Shushtarian, A., 2015. Pore size distribution and methane equilibrium conditions at Walker Ridge Block 313, northern Gulf of Mexico, abstract OS23B-1999, American Geophysical Union Fall Meeting, San Francisco, CA, 15 December 2015.

Clennell, M.B., Hovland, M., Booth, J.S., Henry, P., Winters, W.J., 1999. Formation of natural gas hydrates in marine sediments 1. Conceptual model of gas hydrate growth conditioned by host sediment properties. J. Geophys. Res., 104(B10), 22985-23003.

Cook, A.E., Malinverno, A., 2013. Short migration of methane into a gas hydrate-bearing sand layer at Walker Ridge, Gulf of Mexico. Geochem. Geophys. Geosyst., 14(2), 283-291.

Daigle, H., 2011. Pore-scale controls on permeability, fluid flow, and methane hydrate distribution in fine-grained sediments. PhD thesis, Rice University, Houston, Texas, USA.

Daigle, H., Dugan, B., 2010. Effects of multiphase methane supply on hydrate accumulation and fracture generation. Geophys. Res. Lett., 37, L20301.

Daigle, H., Dugan, B., 2014. Data report: permeability, consolidation, stress state, and pore system characteristics of sediments from Sites C0011, C0012, and C0018 of the Nankai Trough. In: Henry, P., Kanamatsu, T., Moe, K.T., the Expedition 333 Scientists (Eds.), Proceedings of the Integrated Ocean Drilling Program 333. Integrated Ocean Drilling Program Management International, Tokyo, 1-23.

Daigle, H., Screaton, E.J., 2015. Predicting the permeability of sediments entering subduction zones. Geophysical Research Letters 42(13), 5219-5226.

Day-Stirrat, R.J., Flemings, P.B., You, Y., Aplin, A.C., van der Pluijm, B.A., 2012. The fabric of consolidation in Gulf of Mexico mudstones. Marine Geology 295-298, 77-85.

Dutton, S.P., Loucks, R.G., 2014. Reservoir quality and porosity-permeability trends in on shore Wilcox sandstones, Texas and Louisiana Gulf Coast: Application to deep Wilcox plays, offshore Gulf of Mexico. GCAGS Journal 3, 33-40.

England, W.A., MacKenzie, A.S., Mann, D.M., Quigley, T.M., 1987. The movement and entrapment of petroleum fluids in the subsurface. J. Geol. Soc. London, 144, 327-347.

Frye, M., 2008. Preliminary evaluation of in-place gas hydrate resources: Gulf of Mexico Outer Continental Shelf. Minerals Management Service Report 2008-004. Available online at: http://www.boem.gov/uploadedFiles/BOEM/Oil_and_Gas_Energy_Program/Resource_Evaluation/Gas_Hydrates/MMS2008-004.pdf

Gordon, D.S., Flemings, P.B., 1998. Generation of overpressure and compaction-driven fluid flow in a Plio-Pleistocene growth-faulted basin, Eugene Island 330, offshore Louisiana. Basin Res., 10(2), 177-196.

Handa, Y.P., 1990. Effect of hydrostatic pressure and salinity on the stability of gas hydrates. J. Phys. Chem., 94(6), 2652-2657.

Henry, P., Thomas, M., Clennell, M.B., 1999. Formation of natural gas hydrates in marine sediments 2. Thermodynamic calculations of stability conditions in porous sediments. Journal of Geophysical Research 104(B10), 23005-23022.

Hutchinson, D.R., Hart, P.E., Collett, T.S., Edwards, K.M., Twichell, D.C., Snyder, F., 2008. Geologic framework of the 2005 Keathley Canyon gas hydrate research well, northern Gulf of Mexico. Marine and Petroleum Geology 25(9), 906-918.

Liu, X., Flemings, P.B., 2011. Capillary effects on hydrate stability in marine sediments. Journal of Geophysical Research 116, B07102.

Malinverno, A., 2010. Marine gas hydrates in thin sand layers that soak up microbial methane. Earth Planet. Sci. Lett., 292(3-4), 399-408.

Nole, M., Daigle, H., Milliken, K.L., Prodanović, M., 2016. A method for estimating microporosity of fine-grained sediments and sedimentary rocks via scanning electron microscope image analysis. Sedimentology, in press.

Sun, X., Mohanty, K.K., 2006. Kinetic simulation of methane hydrate formation and dissociation in porous media. Chem. Eng. Sci., 61(11), 3476-3495.

Baseline Reporting Quarter	Budget Period 1														
	Q1		Q2		Q3		Q4		Q1		Q2		Q3		Q
	10/1/13 - 12/31/13		1/1/14 - 3/31/14		4/1/14 - 6/30/14		7/1/14 - 9/30/14		10/1/14 - 12/31/14		1/1/15 - 3/31/15		4/1/15 - 6/30/15		7/1/15 -
	Q1	Cumulative Total	Q2	Cumulative Total	Q3	Cumulative Total	Q4	Cumulative Total	Q1	Cumulative Total	Q2	Cumulative Total	Q3	Cumulative Total	Q4
Baseline Cost Plan															
Federal Share	$ 97,167	$ 97,167	$ 97,167	$ 194,333	$ 97,167	$ 291,500	$ 97,167	$ 388,666	$ 97,167	$ 485,833	$ 97,167	$ 582,999	$ 108,258	$ 691,257	$ 108,258
Non-Federal Share	$ 24,292	$ 24,292	$ 24,292	$ 48,583	$ 24,292	$ 72,875	$ 24,292	$ 97,167	$ 24,292	$ 121,458	$ 24,292	$ 145,750	$ 29,698	$ 175,447	$ 29,698
Total Planned	$ 121,458	$ 121,458	$ 121,458	$ 242,916	$ 121,458	$ 364,374	$ 121,458	$ 485,833	$ 121,458	$ 607,291	$ 121,458	$ 728,749	$ 137,956	$ 866,704	$ 137,956
Actual Incurred Cost															
Federal Share	0	0	$ 4,053	$ 4,053	$ 59,844	$ 63,897	$ 135,066	$ 198,963	$ 113,678	$ 312,641	$ 174,686	$ 487,327	$ 36,292	$ 523,619	$ 179,321
Non-Federal Share	0	0	0	0	$ -	$ -	$ 8,832	$ 8,832	$ 63,148	$ 71,980	$ 51,748	$ 123,728	$ 6,615	$ 130,343	$ 21,898
Total Incurred Costs	0	0	0	0	$ 59,844	$ 63,897	$ 143,898	$ 207,795	$ 176,826	$ 384,621	$ 226,435	$ 611,056	$ 42,907	$ 653,963	$ 201,219
Variance															
Federal Share	$ (97,167)	$ (97,167)	$ (93,113)	$ (190,280)	$ (37,323)	$ (227,602)	$ 37,900	$ (189,703)	$ 16,512	$ (173,191)	$ 77,520	$ (95,672)	$ (71,966)	$ (167,638)	$ 71,063
Non-Federal Share	$ (24,292)	$ (24,292)	$ (24,292)	$ (48,583)	$ (24,292)	$ (72,875)	$ (15,460)	$ (88,335)	$ 38,856	$ (49,478)	$ 27,457	$ (22,021)	$ (23,083)	$ (45,104)	$ (7,800)
Total Variance	$ (121,458)	$ (121,458)	$ (117,405)	$ (238,863)	$ (61,614)	$ (300,477)	$ 22,440	$ (278,037)	$ 55,368	$ (222,670)	$ 104,977	$ (117,693)	$ (95,049)	$ (212,742)	$ 63,263

Budget Period 2									Budget Period 3							
4	Q1		Q2		Q3		Q4		Q1		Q2		Q3		Q4	
9/30/15	10/1/15 - 12/31/15		1/1/16 - 3/31/16		4/1/16 - 6/30/16		7/1/16 - 9/30/16		10/1/16 - 12/31/16		1/1/17 - 3/31/17		4/1/17 - 6/30/17		7/1/17 - 9/30/17	
Cumulative Total	Q1	Cumulative Total	Q2	Cumulative Total	Q3	Cumulative Total	Q4	Cumulative Total	Q1	Cumulative Total	Q2	Cumulative Total	Q3	Cumulative Total	Q4	Cumulative Total
$ 799,515	$ 108,258	$ 907,773	$ 108,258	$ 1,016,031	$ 108,258	$ 1,124,289	$ 108,258	$ 1,232,547	$ 111,371	$ 1,343,918	$ 111,371	$ 1,455,290	$ 111,371	$ 1,566,661	$ 111,371	$ 1,678,032
$ 205,145	$ 29,698	$ 234,842	$ 29,698	$ 264,540	$ 29,698	$ 294,237	$ 29,698	$ 323,935	$ 30,888	$ 354,823	$ 30,888	$ 385,711	$ 30,888	$ 416,600	$ 30,888	$ 447,488
$ 1,004,660	$ 137,956	$ 1,142,615	$ 137,956	$ 1,280,571	$ 137,956	$ 1,418,526	$ 137,956	$ 1,556,482	$ 142,260	$ 1,698,741	$ 142,260	$ 1,841,001	$ 142,260	$ 1,983,260	$ 142,260	$ 2,125,520
$ 702,941	$ 142,071	$ 845,012	$ 112,450	$ 957,462												
$ 152,241	$ 21,898	$ 174,139	$ 14,224	$ 188,363												
$ 855,182	$ 163,969	$ 1,019,151	$ 126,674	$ 1,145,825												
$ (96,574)	$ 33,813	$ (62,761)	$ 4,192	$ (58,569)												
$ (52,904)	$ (7,800)	$ (60,704)	$ (15,474)	$ (76,177)												
$ (149,478)	$ 26,014	$ (123,464)	$ (11,281)	$ (134,746)												